Polarimetric Weather Radar Antenna Calibration Using Solar Scans

Richard L. Ice
US Air Force, WSR-88D Radar Operations Center, Norman, Oklahoma
Adam K. Heck, Blake J. McGuire, Lindsey M. Richardson, W. David Zittel, Robert R. Lee
US National Weather Service, WSR-88D Radar Operations Center, Norman, Oklahoma
Jeffrey G. Cunningham, Air Force Weather Agency

1. INTRODUCTION

The US Next Generation Weather Radar (NEXRAD) program operates and maintains the Nation's Doppler weather radar network in support of the National Weather Service, the Federal Aviation Agency, and the Department of Defense. The radar is designated the Weather Surveillance Radar – 1988 Doppler (WSR-88D). The system has been in operation since the early 1990's (Crum, 1993), and has been continuously upgraded to infuse new technology and to enhance capability (Vogt, 2011). The radar is not only critical for supporting weather forecast and warning operations, but has found many other scientific uses including ornithological research (Diehl, 2005). This report by the US Forest Service, which is focused on the use of the radar for tracking bird migration, is a good overview of the radar and contains detailed descriptions of the basic products available from the WSR-88D.

The most recent improvement has been an expansion to dual polarimetric capability (Saxion, 2011). This added a second linearly polarized transmission and reception feature. The system now simultaneously transmits signals featuring the electric component of the EM wave with linear horizontal (H) and linear vertical (V) polarizations. By comparing the relative return powers from the H and V channels, tracking the relative phases of the return signals, and measuring how well they are correlated, the system provides detailed information on the types of hydrometeors that make up the radar resolution volume. This aspect greatly improves radar estimated rainfall rates and can accurately identify the type of precipitation.

Unlike surveillance and aircraft tracking radars, which are focused on probability of detection, weather radars must be able to make accurate measurements of the return signals. The power returned is directly related to the strength of the weather contained in the radar resolution volume. The precision with which the radar can estimate rain rates is directly related to the ability of the system to relate return power measurements to the meteorological phenomena. Measured return powers are translated into meteorological variable estimates. An estimate accuracy of 1 dB is required in order to support good precipitation estimation performance. More precisely, this power is related to the meteorological parameter of reflectivity factor (Z) which is normally expressed in logarithmic units (dBz, Smith 2010) due to the wide dynamic range of the measurements. This important parameter is obtained by converting the power measured by the radar receiver and signal processor into meteorologically relevant values through the weather radar equation [6].

$$P(\mathbf{r}_0) = \frac{\pi^3 P_t g^2 g_S \theta_1^2 c \tau |K_W|^2 Z_e}{2^{10} (\ln 2) \lambda^2 r_0^2 l^2 l_r}$$

In this relation, which is equation 4.34 from [6], the received power $P(\mathbf{r}_0)$ is related to the reflectivity factor Z_e by multiple parameters such as receiver gain (g_s), system losses (l), transmitter power (P_t), etc. The process of calibration determines the values of these parameters, and as previously described, the measurements must yield a total power measurement accuracy of 1 dB or less for satisfactory performance. Meeting this requirement for a large network of radars (over 160 units) has proven to be challenging and a number of papers have addressed this issue (Ice, 2005; Gourley, 2003; Atlas, 2002).

The factor g in the equation is the one-way antenna gain and θ_1 represents the antenna half power beamwidth. Because meteorological radars use pencil beam patterns, antennas are designed such that the azimuth and elevation planes of the pattern have equal widths. Note that both gain and beamwidth are squared factors due to the combination of transmit and receive operations in the same antenna. Solar scans form the basis for antenna calibration in the WSR-88D. For the WSR-88D antenna, solar scans are used for calibration.

2. BASIC USES OF THE SUN IN THE WSR-88D

The WSR-88D antenna (Figure 1) is a center fed parabolic reflector. Figure 2 shows the relevant dimensions and design parameters. The nearly 28 foot diameter dish provides about 45 dB of gain at the nominal 10 cm operating wavelength (S-band) and features a 3 dB beamwidth of less than 0.95 degrees and very low sidelobes. The Appendix contains a typical example of the pattern. While most of the radar system parameters needed for calibration can be measured with test equipment or built-in hardware sub-systems, accurately measuring the antenna gain and beamwidth is a challenge due to the large physical size. Because the operational units are housed within radomes, the effects of which must be included in gain measurements, this leads to a further need to measure the antenna parameters in the field.

* Corresponding Author Address: Richard L. Ice, US Air Force., WSR-88D Radar Operations Center, 1313 Halley Circle. Norman, OK, 73069

e-mail: Richard.L.Ice@noaa.gov

The views expressed are those of the authors and do not necessarily represent those of the United States Air Force.

Figure 1. The WSR-88D Antenna

Antenna gain and beamwidth parameters could be obtained by use of external signal generators and test antennas, essentially establishing each WSR-88D location as a non-ideal antenna test range. However there are logistical and technical challenges to this approach. Other external approaches such as calibration spheres have been proposed and tested (Ice, 2005; Atlas, 2002). But these also present serious logistical challenges. There is a need for a stable, reliable, and well understood external target for measuring the antenna characteristics. The sun is an excellent external target for characterizing radar systems because its position is well known on a real time basis through astronomical calculations, and its microwave transmission characteristics are well understood and monitored multiple times each day by the space weather community (Tapping, 2001).

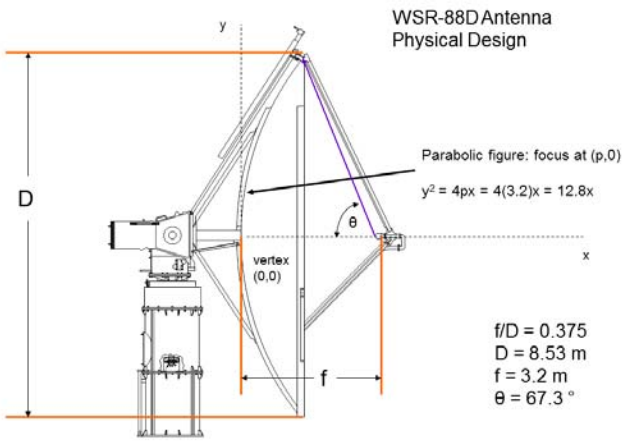

Figure 2. The WSR-88D Antenna Specifications

The original solar scan approach for the WSR-88D derived three system parameters: antenna beam axis position correction, antenna pattern beamwidth, and antenna gain. These methods consist of two operations, or sub-tests (Free, 2007). Subtest 1 scans the antenna main beam 3 degrees about the expected location of the sun in azimuth and elevation while the sun passes through the antenna main lobe due to the motion of the earth. Once the noise powers of the solar signal have been collected, the software creates a plot of power as a function of angle, both in azimuth and elevation, where the angles are those reported by the pedestal control electronics. The software then fits a parabolic curve to the power data, finds the peak, and compares that peak to the elevation and azimuth of the expected position of the sun at the associated time, based on a precise astronomical model. The difference in the position of the measured peak and the expected position of the sun is the error in antenna positioning due to misalignment of the antenna and the control electronics. These error correction factors are presented to the radar operator or technician and can be used to refine the accuracy of antenna positioning. The 3 dB beamwidth is also derived from this curve fit process. Figure 3 is a sample of a plot presented to the technician for quality control purposes. The plot shows the noise power of the sun as a function of azimuth as the antenna scans the calculated position of the sun. The parabolic curve is the result of the fit to the data samples. The peak of the fitted curve is compared to the expected center of the sun at the time of the samples and a positioning correction can then be applied.

This method can be subject to error, particularly if electromagnetic interference is present at the time of the solar scan. The curve fit routine may include points from sources other than the solar noise power since the nominal signal-to-noise ratios from the sun's noise power are between 10 and 15 dB. The quality check display of Figure 3 will be a new addition to the technician's tool box. Technicians will be advised to accept results for position correction and beamwidth only if the goodness of fit of the curve is 0.98 or better.

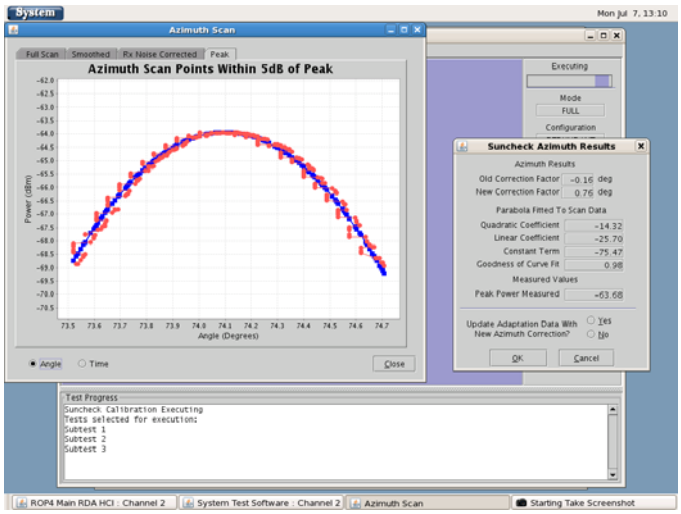

Figure 3. Curve Fit Quality Check Display

The antenna gain is found by comparing the integrated noise power as seen by the radar to the expected noise power of the sun derived from observations at solar observatories (Tapping, 2001). The accuracy of this measurement depends highly on the results of the position error tests. Because the sun's

microwave band image subtends an angle of just over 0.5 degrees, and the antenna beamwidth is less than 0.95 degrees, matching the solar disk to the main lobe of the antenna pattern is important. Figure 4 shows the microwave band solar noise power across the solar disk (Kennewell, 1989).

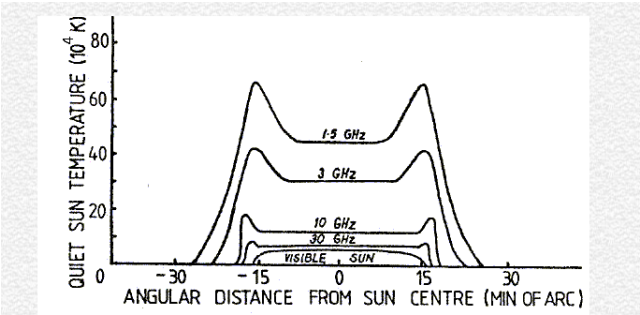

Figure 4. Sun Temperature at Microwave Frequencies

As seen for the frequency close to the WSR-88D band (2.7 to 3.0 GHz), the noise power has peaks at 15 arc minutes from the solar center, thus spanning at least 0.5 degrees. There is some power even beyond that range, approaching a total of 60 arc minutes, or a full degree. An image of the sun's emissions in the bandwidth of the WSR-88D is shown in Figure 5. The colors represent the noise power in the horizontal channel as seen by the radar receiver and signal processor as the beam is scanned in a two dimensional pattern over the solar disk. The peak power seen in the center is about -65 dBm. In this case the signal to noise ratio is around 20 dB as the nominal Intermediate Frequency (IF) stage noise level in the digital receiver is -85 dBm.

The technicians obtain the solar flux information from the observatories when conducting a sun scan for measuring gain. The observatory measurements are made no more frequently than three times per day, so it is important to obtain the most current data. In periods of quiet sun, where solar activity is low, this is not critical. During outbreaks of solar flares, when the flux can vary over a few hours, errors can occur if the solar data is not current.

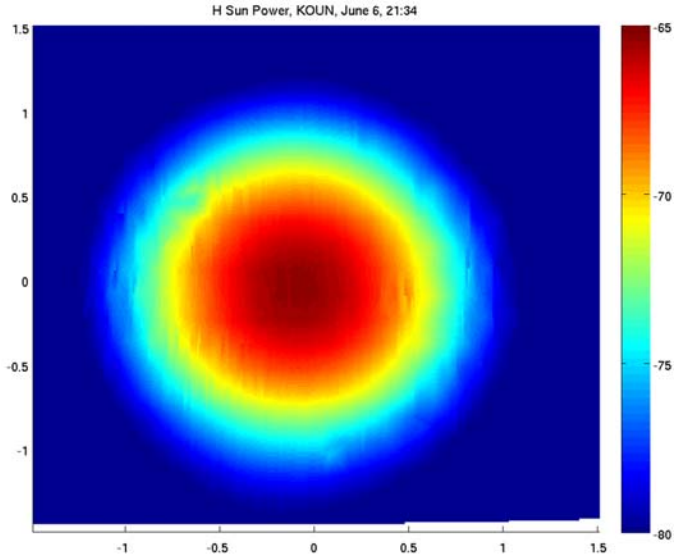

Figure 5. Solar Noise Signal Power

3. POLARIMETRIC CRITICAL MEASUREMENTS

The dual-polarization upgrade further drove calibration accuracy requirements. The power difference between the H and V channels must be measured to within a tolerance of 0.1 dB and the antenna parameters are critical, especially the differential gain and the cross-polarization isolation (Zrnic, 2010). This power is used to extract the differential reflectivity analogous to the reflectivity obtained from a single polarization return. To obtain the bias component of differential reflectivity due to the antenna, the gains of the H and V channel of the antenna are derived from the solar scans, in effect making two gain measurements. The sun's microwave emissions are considered un-polarized, so the expected value of differential reflectivity from the sun is zero. As noted before, positioning the antenna beam center accurately on the center of the solar disk is very important. If the beam is off center either in elevation or azimuth, the measurement yields an unacceptable bias. Figure 6 shows this differential power measurement (H – V) across the solar disk obtained by scanning the antenna in two dimensions over a wide angle. This plot spans 3.0 degrees, encompassing the combined antenna pattern and solar disk extent. Blue colors represent a difference of 0 dB while dark red is for a difference of 0.7 dB.

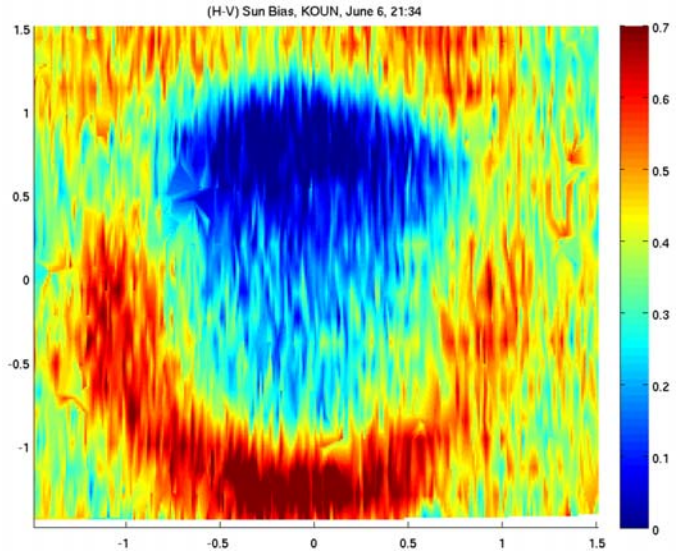

Figure 6. Differential Power Across the Solar Disk

Note that the difference is low near the sun's center while it increases towards the edge. This departure from zero is due to the mismatch of the antenna beam to the solar disk which leads to errors in the antenna bias measurement. Technicians are instructed to obtain satisfactory antenna position correction results prior to running the antenna bias test.

4. LONG TERM MONITORING

The daily sunrise and sunsets can be used to monitor the state of the radar, both for positon accuracy of the pedestal control mechanism as well as for the differential reflectivity bias measurement. Early results with the dual-polarization deployment and analysis of calibration performance have highlighted the need for continuous monitoring with external targets (Cunningham, 2013). Engineers and scientists in the

program have implemented methods for finding the daily sun spikes associated with the sunrise and sunset when seen by the radar (Zittel, 2014).

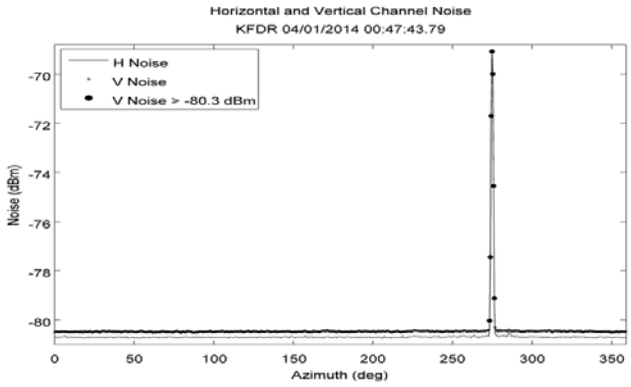

Figure 7. Noise Spike from Antenna Intercepting the Sunset.

These serendipitous measurements can be used to track positon accuracy as well as the differential reflectivity bias of the total receive path of the radar system. Figure 7 shows the noise power seen in both the H and V channels as the antenna scans 360 degrees and intercepts a sunset. The software monitoring the position accuracy can identify the radial containing the peak sun noise power and compare the reported position to the expected location of the sun from astrophysical computations.

The software can further estimate the differential power at the peak using the aforementioned assumption of the sun being un-polarized. The difference between the expected and observed positon of the sun and the difference in power between H and V channels can be analyzed in a scatterplot. Figure 8 shows examples of this analysis for two radar systems.

Each dot represents a sunspike measurement. The position of the dot is the error (in azimuth and elevation) derived from comparing the observed location of the sunspike maximum with the expected location. The many dots represent long term accumulation of these daily measurements. Since the radial data is presented in 0.5 degree increments, the sun power maximum does not always fall exactly in the center of the radial containing the maximum power. Therefore a small error exists for each observation. However, over time the random nature of the measurement results in averaging out these errors. The performance of the radar can be derived from observing the symmetry of how the dots scatter about zero. If the scattered dots are not centered on zero, then the radar beam must contain a pointing error. Note that in the top panel of Figure 8, the dots are centered about zero, while in the bottom panel, there appears to be a pointing error in elevation.

The color of each dot represents the bias error in the differential reflectivity. This estimation is possible because the expected value of differential reflectivity is zero since the sun is un-polarized. As expected, the mean value of the differential reflectivity in the lower panel is biased, having a mean value of -0.72 dB. The mean values in the top panel are close to zero, likely because the antenna pointing is accurate and the resulting antenna bias measurements from the off-line solar scans yielded good results. This approach, developed in the international community recently, shows great promise for routine monitoring of polarimetric radar health and status (Holleman, 2010).

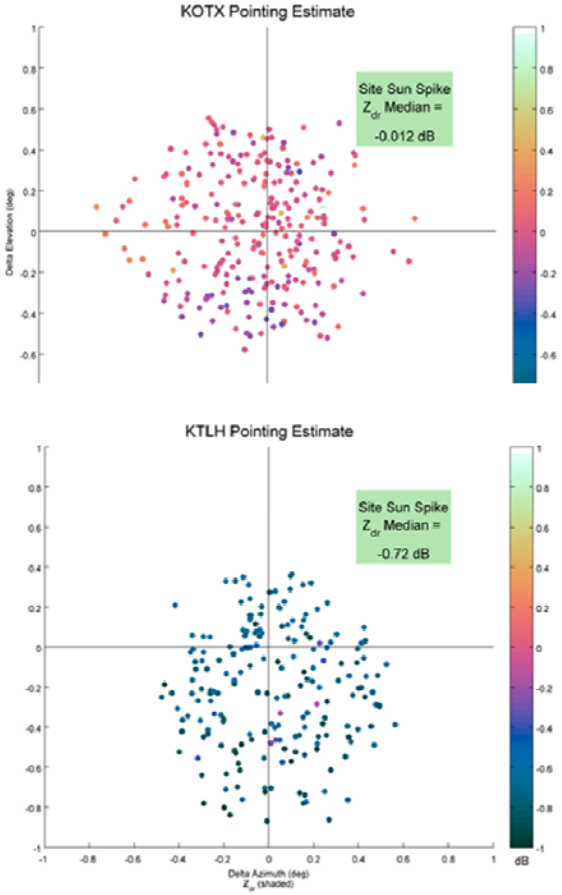

Figure 8. Sunspike Monitoring for Two Radars

5. FUTURE PLANS FOR SOLAR SCANNING

The WSR-88D solar scanning process has seen some recent improvements, mostly aimed at identifying when the antenna is not pointing directly at the center of the solar disk. This is done by instituting strict quality standards on the positon curve fit process during the azimuth and elevation scans of the predicted sun position. A more robust approach comes with full two-dimensional scanning of the sun. These “box scans” move the antenna beam center over a wider window of elevation and azimuth dimensions while following the sun in its course over the sky. The result is a two dimensional analysis as seen in Figures 5 and 6. By capturing a wide image of the microwave power of the solar disk, errors in pointing the antenna are no longer a critical element. The center of the sun can be retrieved by locating the centroid of power and the beam width can be computed from the shape of the power as a function of distance from the center. The differential reflectivity

bias can be found by integrating the powers from the H and V scans over the full disk.

The engineering and science teams with the NEXRAD program are working to develop the box scan as a replacement for the simple separate azimuth and elevation scans, eliminating the need for the more error-prone curve fitting process. This method, along with the daily monitoring of sunspikes, should lead to more accurate differential reflectivity calibration and reduced errors in radar derived precipitation measurements.

REFERENCES

T. D. Crum and R. L. Alberty, 1993, The WSR-88D and the WSR-88D Operational Support Facility, *Bulletin of the American Meteorological Society*, **74**, No. 9.

R. J. Vogt, T. Crum, J. Chrisman, J. Reed, M. Istok, B. Saffle, D. Melendez, D. Forsyth and K. Kelleher, 2011, The WSR-88D: Still the Best and Getting Better, *27th International Conference on Interactive Information Systems Processing for Meteorology, Oceanography, and Hydrology*.

R. H. Diehl and R. P. Larkin, 2005, Introduction to the WSR-88D (NEXRAD) for Orinthological Research, USDA Forest Service General Technical Report PSW-GTR-191.

D. S. Saxion, R. L. Ice, O. E. Boydstun, J. N. Chrisman, A. K. Heck, S. D. Smith, W. D. Zittel, A. D. Free, M. J. Prather, J. C. Krause, P. T. Schlatter, R. W. Hall, and R. D. Rhoton, 2011, "New Science for the WSR-88D: Validating the Dual Polarization Upgrade, *27th International Conference on Interactive Information Systems Processing for Meteorology, Oceanography, and Hydrology*.

P. L. Smith, 2010, The Unit Symbol for the Logarithmic Scale of Radar Reflectivity Factors, *Journal of Atmospheric and Oceanic Technology*, **27**, 615 – 616.

R. J. Doviak and D. S. Zrnic, 1993, Doppler Radar and Weather Observations, 2nd Ed., Academic Press.

R. L. Ice, D. A. Warde and F. Pratte, 2005, Exploring External and Dual Polarization Options for the WSR-88D, *32nd Conference on Radar Meteorology*.

D. Atlas, Radar Calibration, Some Simple Approaches, 2002, *Bulletin of the American Meteorological Society*, **83**, No. 11.

J. J. Gourley, B. Kaney, and R. A. Maddox, 2003, Evaluating the Calibrations of Radars: A Software Approach, *31st Conference on Radar Meteorology*.

K. Tapping, 2001, Antenna Calibration Using the 10.7 cm Flux, Proceedings of the American Meteorological Society Workshop on Radar Calibration, Albuquerque, NM.

A. D. Free, N. K. Patel, R. L.Ice and O. E. Boydstun, 2007, WSR-88D antenna Gain and Beamwidth Algorithms, *23rd International Conference on Interactive Information Systems Processing for Meteorology, Oceanography, and Hydrology*.

J. A. Kennewell, 1989, Solar Radio Interference to Satellite Downlinks, *6th International Conference on Antennas and Propagation* IEEE ICAP89, 334 – 339.

D. Zrnic, R. Doviak, G. Zhang and A. Ryzhkov, 2010, Bias in Differential Reflectivity due to Cross Coupling through the Radiation Pattern of Polarimetric Weather Radars, *Journal of Atmospheric and Oceanic Technology*, **27**, 1624 – 1637.

J. G. Cunningham, W. D. Zittel, R. R. Lee, R. L. Ice and N. P. Hoban, 2013, Methods for Identifying Systematic Differential Reflectivity (Zdr) Biases on the Operational WSR-88D Network, *36th Conference on Radar Meteorology*.

W. D. Zittel, J. G. Cunningham, R. R. Lee, L. M. Richardson, R. L. Ice and V. Melnikov, 2014, Use of Hydrometeors, Bragg Scatter, and Sun Spikes to Determine System ZDR Biases in the WSR-88D Fleet, *8th European Conference on Radar in Meteorology and Hydrology*.

I. Holleman, A. Huuskonen, R. Gill, P. Tabary, 2010, Operational Monitoring of Radar Differential Reflectivity Using the Sun, *Journal of Atmospheric and Oceanic Technology*, **27**, 881-887

Appendix – WSR-88D Antenna Pattern, (with radome and prototype polarimetric feed)

Obtained with non-ideal range testing in Norman Oklahoma, (note enhanced sidelobes from nearby objects)

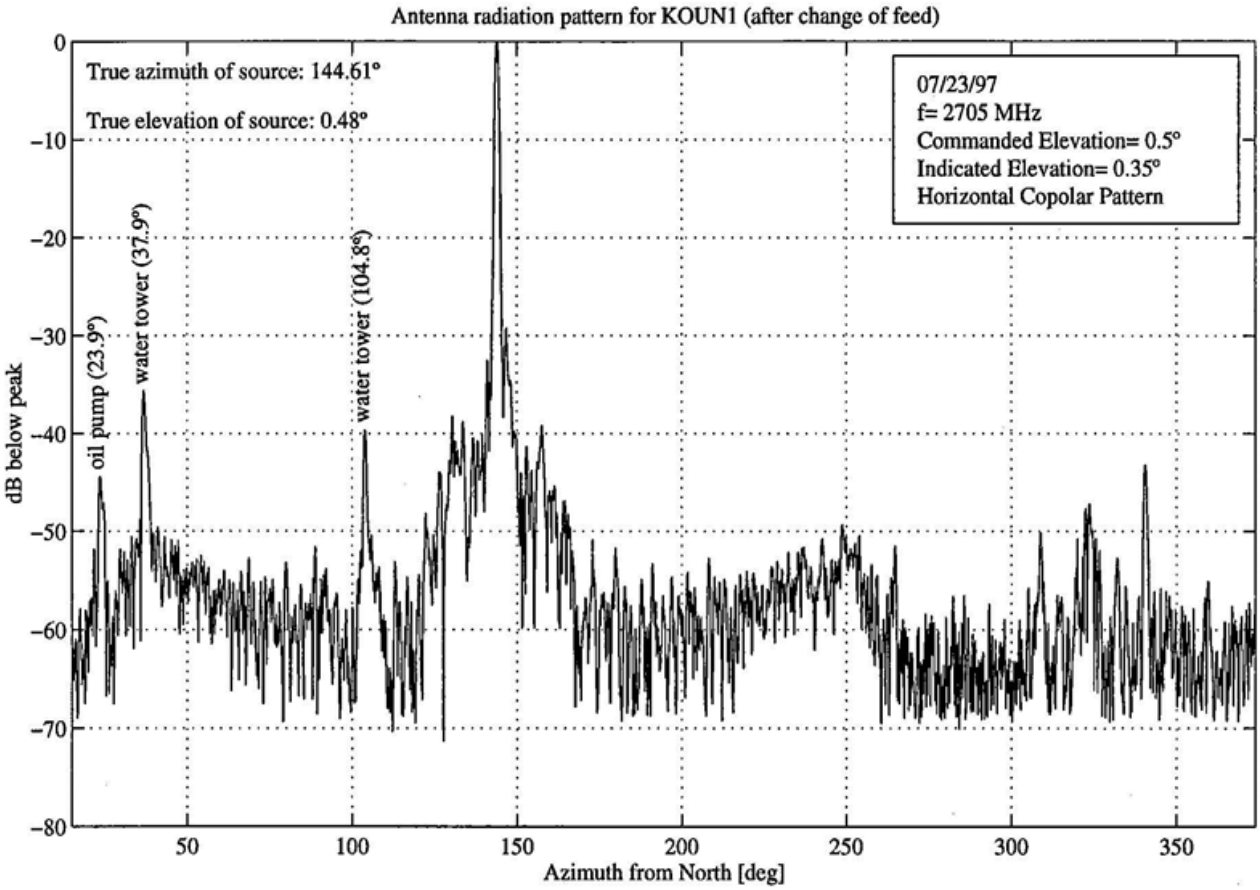

Source: Doviak, R. J., and D. Zrnic´ , Polarimetric upgrades to improve
Rainfall measurements, NOAA/NSSL Tech. Rep., 110 pp.
[Available online at http://www.nssl.noaa.gov/publications/wsr88d_reports/2pol_upgrades.pdf.]